Effect of Precipitation on the Mechanical Response of Cu–3Ag–0.6Zr Alloy during Hot Compression

Zhiyong XUE[1, a*], Lingyun GU[1, b], Yu REN[1, c], Xiaoyang HAO[1, d] and Ping XU[1, e]

[1]School of energy, power and mechanical engineering, North China Electric Power University, Beijing 102206, PR China

[a]xuezy@ncepu.edu.cn, [b]cloudgly@126.com, [c]renyu@ncepu.edu.cn,
[d]13269501803@163.com, [e]453544515@qq.com

Abstract. Hot compression experiments were conducted on a Cu–Ag–Zr alloy with low Ag content, Cu–3Ag–0.6Zr, to investigate the effect of precipitation on the mechanical response of this alloy. The results show that the stress-strain behavior of Cu–3Ag–0.6Zr alloy is significantly affected by the precipitation. The flow stress of the alloy deformed at temperatures of 623–673 K and a strain rate of 10^{-3} s^{-1} increases due to the occurrence of the continuous and discontinuous precipitation. However, the precipitation process is suppressed with increasing strain rate, resulting in almost identical flow stress of the alloy deformed at different temperatures.
Keywords: Cu–3Ag–0.6Zr alloy; Precipitation; Stress-strain behavior; Microstructure evolution

1 Introduction

Cu–Ag–Zr alloys with low Ag contents have been considered for aerospace application such as the thrust chamber of liquid rocket engine because of their high thermal conductivity [1]. For this application, Ag is considered as a strengthening element, and the addition of Zr enhances the formation of precipitates, which can also improve the strength level of copper alloys [2, 3]. Additionally, the small amounts of Zr also play a role as a grain refinement and getter for soluble oxygen [4]. NARloy-Z is one such alloy designed to manufacture the combustion chamber liner of liquid rocket engine [4, 5]. Some studies have focused on the microstructure evolution and its effect on the mechanical properties of Cu–Ag–Zr alloys [1, 6]. Krishna et al. [1] observed uniformly distributed fine nanocrystalline Ag precipitates in the NARloy-Z after aging at 723 K. The results of the subsequent tensile test revealed that the yield and ultimate tensile strength of the aged NARloy-Z were increased, indicating the strengthening effect of these precipitates. However, when tested at elevated temperatures, the ultimate tensile strength of the aged NARloy-Z is lower than that of the solution-treated material. Jia et al. [6] researched the aging hardening behavior of Cu–0.1Ag–0.2Zr alloy.

* Corresponding author: xuezy@ncepu.edu.cn

They found that the Cu_5Zr with FCC structure precipitates during aging at 723 K, which leads to a significant increase in the hardness of the alloy. However, the effect of precipitation on the mechanical response of Cu–3Ag–0.6Zr alloy during hot compression have not yet been extensively studied, which is a basis for its hot working process design.

In the present study, the precipitation behavior and its effect on the mechanical properties of one particular Cu–Ag–Zr alloy, Cu–3Ag–0.6Zr, were investigated through compression tests carried out with various strain rates at different deformation temperatures. The stress-strain behavior of this alloy was analyzed. The microstructure evolution during hot deformation was also examined.

2 Experimental Procedure

The ternary Cu–3Ag–0.6Zr (wt.%) alloy investigated was prepared by induction melting. Then the ingot was forged at the temperature range of 1073–923 K. A block with dimensions of 100 mm × 100 mm × 40 mm was cut from the forged piece, and then solution treated (ST) at 1193 K for 40 min and water quenched. The cylindrical specimens with 8 mm diameter and 12 mm height for hot compression tests were machined from the ST block. The microstructure of the ST material consists of equiaxed grains with some annealing twins. The grain size of the alloy in the ST state was measured to be about 87 μm.

Hot deformation experiments were carried out on a Gleeble-3800 thermal simulator at the deformation temperature range of 573–723 K and strain rate range of 10^{-3}–1 s^{-1}, respectively, up to a total deformation of 50% (i.e., the true strain is about 0.693). The sample was resistance heated to deformation temperature at a heating rate of 10 K/s and held for 180 s before compression.

In order to retain the deformed microstructures, the cylinders were water quenched upon completion of the compression tests. Then the deformed microstructures were examined using a ZEISS Axio Observer A1m optical microscope (OM) and a Hitachi S-4800 field-emission scanning electron microscope (FESEM) equipped with OXFORD energy dispersive spectroscope (EDS). For microstructure observation, the specimens were mechanically polished followed by etching in a solution of 5 g $FeCl_3$ + 20 ml HCl + 100 ml H_2O at room temperature. To show the change in the substructure of the alloy deformed at different temperatures and strain rates, TEM analyses were conducted using a TECNAI G2 F30 system at an accelerating voltage of 300 kV. For the TEM observations, thin samples with an initial thickness of 0.5 mm were cut from the cylinders after OM and SEM examinations, firstly reduced to less than 50 μm thick by mechanical means, then punched into several standard 3 mm diameter TEM discs, and finally thinned by ion milling.

3 Results

3.1 Stress-strain Behavior of Cu–3Ag–0.6Zr Alloy.

Typical true stress-strain curves obtained during hot compression of the Cu–3Ag–0.6Zr alloy with various strain rates at different deformation temperatures are shown in Fig. 1. Overall, the flow stress increases with increasing strain (except for the case at 10^{-3} s^{-1} and at 723 K), as shown in Fig. 1, indicating a significant strain hardening effect. However, the stress-strain behavior markedly changes when the strain rate increases. Fig. 1(a) shows that, under a loading strain rate of 10^{-3} s^{-1}, the flow stress at 623 K is higher than that at 573 K after the strain exceeding about 0.2. When the temperature increases to 673 K, the flow stress of the

alloy is approximately equal to that at 573 K. The flow stress dramatically drops as the temperature further increases to 723 K. When the strain rate rises to 10^{-2} s^{-1} (Fig. 1(b)), the gap between the stress-strain curves obtained at different temperatures reduces. The flow stress at 623 K and at 673 K is still higher than that at 573 K. The flow stress at 723 K increases and also becomes higher than that at 573 K before the strain exceeding about 0.6. When the strain rate further increases (Fig. 1(c) and (d)), the stress-strain curves gradually close to and finally overlap each other.

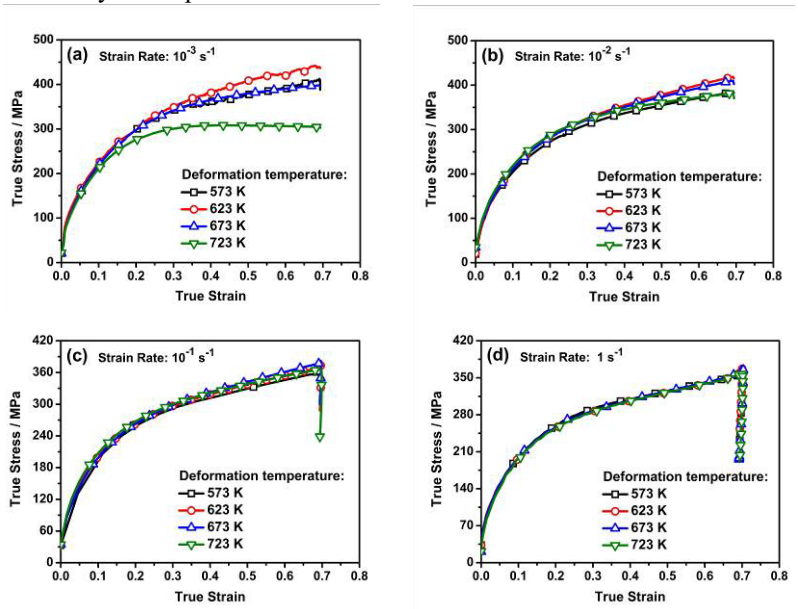

Fig. 1. Typical true stress-strain curves of the alloy compressed at 573–723 K with a strain rate of: (a) 10^{-3} s^{-1}, (b) 10^{-2} s^{-1}, (c) 10^{-1} s^{-1}, (d) 1 s^{-1}.

3.2 Microstructural Characteristics.

Figure 2 shows the microstructures of the Cu–3Ag–0.6Zr alloy deformed at 623 K under different strain rates. The grains are elongated to some extent at a strain rate of 10^{-3} s^{-1} (Fig. 2(a)). In addition, many secondary phase particles are observed. Most of the dark particles discretely distribute at grain boundaries and twin boundaries. The mean size of this secondary phase is approximately 11.4 μm. Some fine particles are arranged in chain-like conformation (indicated by the arrows). Under the strain rates higher than 10^{-3} s^{-1} (Fig. 2(b) and (c)), the hot deformed microstructure of this alloy is still comprised of elongated grains and secondary phase particles distributed at grain boundaries and twin boundaries. Chain-like distributed fine particles are also observed (Fig. 2(b)). The mean size of the secondary phase particle hardly changes with increasing strain rate and is about 11.8 and 10.8 μm at a loading strain rate of 10^{-2} s^{-1} and 10^{-1} s^{-1}, respectively. However, the number of particles gradually reduces with increasing strain rate.

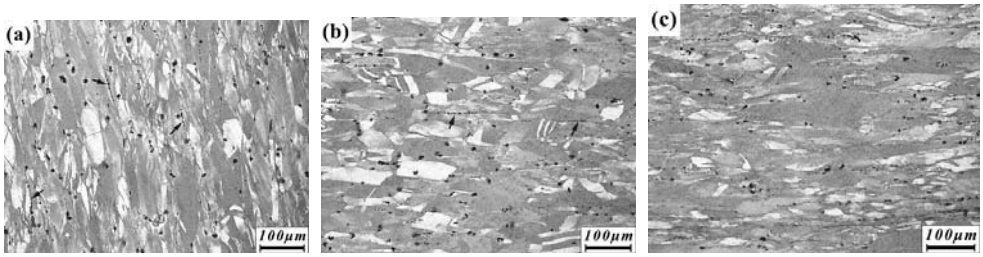

Fig. 2. Microstructures of the alloy deformed at 623 K with a strain rate of: (a) 10^{-3} s^{-1}, (b) 10^{-2} s^{-1}, (c) 10^{-1} s^{-1}.

Figure 3 shows the microstructures of the Cu–3Ag–0.6Zr alloy deformed at 723 K. The deformed grains and some secondary phase particles distributed at grain boundaries are also observed in the alloy compressed at this temperature, as shown in Fig. 3(a). Moreover, some fine equiaxed grains distributed along grain boundaries and around dark particles (indicated by the circles) are observed, which indicates the occurrence of the dynamic recrystallization. When the strain rate further increases (Fig. 3(b) and (c)), the grains are elongated more seriously and the number of secondary phase particles reduces. The mean size of the particle is approximately 7.8, 8.8 and 7.6 μm at a strain rate of 10^{-3} s^{-1}, 10^{-2} s^{-1} and 10^{-1} s^{-1}, respectively, which is somewhat less than that in the alloy deformed at 623 K. The number of these particles is also less than that at 623 K, suggesting the suppression of the precipitation. In addition, the secondary phase particles are distributed more discretely and no chain-like arranged fine particles are observed in the alloy compressed at 723 K.

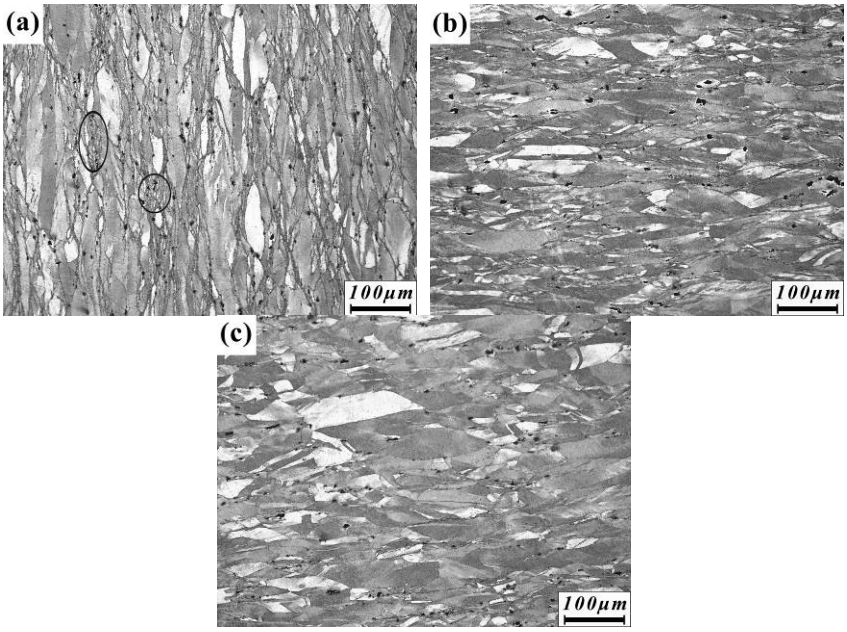

Fig. 3. Microstructures of the alloy deformed at 723 K with a strain rate of: (a) 10^{-3} s^{-1}, (b) 10^{-2} s^{-1}, (c) 10^{-1} s^{-1}.

4 Discussion

In-situ aging occurs during hot compression at 573–723 K, resulting in the formation of various precipitates in Cu–3Ag–0.6Zr alloy. Some precipitates nucleate at grain boundaries or twin boundaries (Fig. 2 and 3), which are known as the discontinuous precipitates [7]. Figure 4 shows the scanning electron micrographs and corresponding EDS spectra of these discontinuous precipitates in the alloy after compression at 623 K. Two types of discontinuous precipitates were observed, namely large white particle (7.6–11.8 μm, Fig. 4(a)) and small gray particle (0.8–2 μm, Fig. 4(b)). The large particles were broken up during the preparation of the specimens for microstructure observation. Even so, some qualitative analysis can be done on the residues of these particles. EDS analysis results show that the large white particles are the Ag-rich phase and the small gray particles are the Cu–Ag–Zr intermetallic phase. These coarse secondary phases form because of very low solubility of Ag and Zr in the copper matrix and restrict the grain growth during the hot compression process by pinning the grain boundaries. In addition, there is a peak of oxygen in front of the predominant peak of Cu in the EDS spectrum of the intermetallic phase (Fig. 4(b)). This observation confirms that Zr plays a role as an oxygen fixer [4]. However, the discontinuous precipitation is suppressed by adding Zr element, and the limited number of coarse secondary phases should not have a significant effect on the stress-strain behavior of Cu–3Ag–0.6Zr alloy.

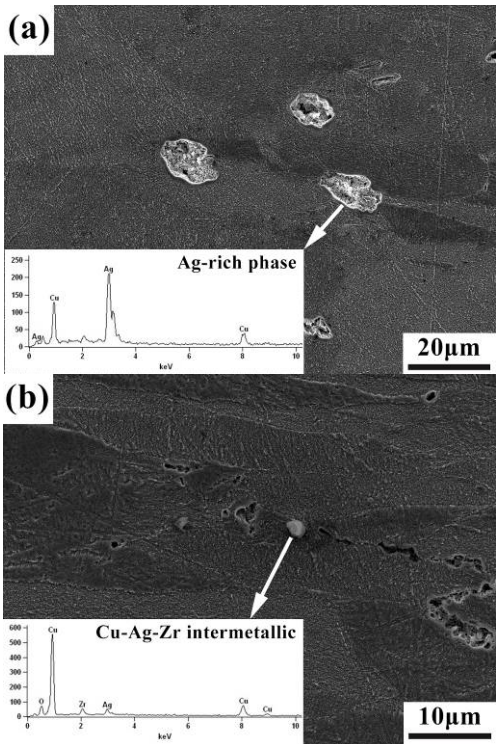

Fig. 4. SEM micrographs and corresponding EDS spectra of the discontinuous precipitates in the alloy deformed at 623 K with a strain rate of 10^{-3} s^{-1}: (a) Ag-rich phase and (b) Cu–Ag–Zr intermetallic phase.

In addition to some relatively large discontinuous precipitates, a mass of nanocrystalline precipitates were also observed in the hot deformed alloy, as shown in Fig. 5(a). These fine

precipitates are spherical and distribute uniformly in the Cu matrix, which are known as the continuous precipitates [8]. The average size of the nanocrystalline precipitates was measured to be about 16.8 nm. The EDS spectrum (Fig. 5(b)) shows prominent silver peaks with some peaks of copper confirming that the precipitates are of pure silver. These continuous Ag precipitates are responsible for the enhanced strength in the aged Cu–Ag alloys.

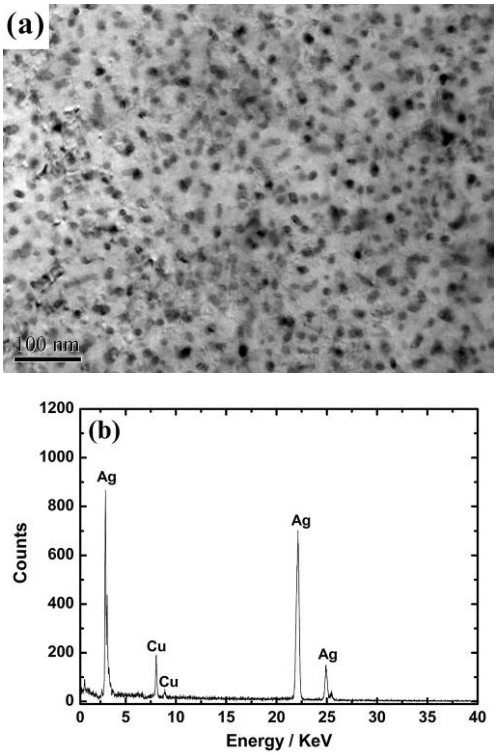

Fig. 5. (a) TEM image and (b) corresponding EDS spectrum of the continuous Ag precipitates in the alloy deformed at 623 K with a strain rate of 10^{-3} s^{-1}.

These continuous precipitates also should play a very important role in the strengthening of Cu–3Ag–0.6Zr alloy during hot deformation. At a low strain rate, a good deal of nano scale Ag precipitates form when the alloy deforms at 623 K, resulting in the highest flow stress (Fig. 1(a)). When the deformation temperature rises, the thermal softening effect gradually increases and counteract the strengthening effect caused by precipitation, leading to the decrease in flow stress of the alloy. As the temperature further increases to 723 K, the dynamic recrystallization takes place (Fig. 3(a)), which brings about the significant decrease in flow stress (Fig. 1(a)). High strain rate means short time for deformation as well as precipitation. The number of the continuous precipitates is likely to reduce when the alloy deforms at a strain rate higher than 10^{-3} s^{-1}. So the strengthening effect resulting from the continuous precipitation is weakened and the stress-strain curves gradually closes to each other as the strain rate increases. However, the dynamic recrystallization process is also suppressed under high strain rate deformation conditions, so the flow stress of the alloy deformed at 723 K increases with increasing strain when the strain rate reaches and exceeds 10^{-2} s^{-1}.

5 Summary

A series of hot compression experiments were carried out on samples of the Cu–3Ag–0.6Zr alloy to investigate the effect of precipitation on the mechanical response of this alloy. The stress-strain behavior of Cu–3Ag–0.6Zr alloy is significantly affected by the occurrence of precipitation which depends on the deformation temperatures and loading strain rates. At a temperature range of 623–673 K, abundant continuous precipitates and some discontinuous precipitates form under a low strain rate (10-3 s^{-1}) condition, leading to increased flow stress of the alloy. However, the precipitation process is suppressed with increasing strain rates, resulting in almost identical flow stress of the alloy deformed at different temperatures. When the alloy deforms at 723 K and at 10^{-3} s^{-1}, the flow stress dramatically drops due to the thermal softening caused by dynamic recrystallization.

Acknowledgment

This study was financed by the Program for New Century Excellent Talents in University (NCET-12-0849) and the Fundamental Research Funds for the Central Universities (2014ZZD03 and 13ZD12).

References

1. S. C. Krishna, K. T. Tharian, B. Pant, R. S. Kottada, Microstructure and mechanical properties of Cu-Ag-Zr alloy, J. Mater. Eng. Perform. 22 (2013) 3884-3889.
2. A. Gaganov, J. Freudenberger, E. Botcharova, L. Schultz, Effect of Zr additions on the microstructure, and the mechanical and electrical properties of Cu–7 wt.%Ag alloys, Mater. Sci. Eng. A 437 (2006) 313-322.
3. J. Lyubimova, J. Freudenberger, C. Mickel, T. Thersleff, A. Kauffmann, L. Schultz, Microstructural inhomogeneities in Cu–Ag–Zr alloys due to heavy plastic deformation, Mater. Sci. Eng. A 527 (2010) 606-613.
4. J. Singh, G. Jerman, R. Poorman, B. N. Bhat, A. K. Kuruvilla, Mechanical properties and microstructural stability of wrought, laser, and electron beam glazed NARloy-Z alloy at elevated temperatures, J. Mater. Sci. 32 (1997) 3891-3903.
5. J. H. Sanders, P. S. Chen, S. J. Gentz, R. A. Parr, Microstructural investigation of the effects of oxygen exposure on NARloy-Z, Mater. Sci. Eng. A 203 (1995) 246-255.
6. S. G. Jia, X. M. Ning, P. Liu, M. S. Zheng, G. S. Zhou, Age Hardening Characteristics of Cu-Ag-Zr Alloy, Met. Mater. Int. 15 (2009) 555-558.
7. I. Manna, S. K. Pabi, A study of the nucleation characteristics of discontinuous precipitation in a pro-eutectic Cu-Ag alloy, J. Mater. Sci. Lett. 9 (1990) 1226-1228.
8. F. Bittner, S. Yin, A. Kauffmann, J. Freudenberger, H. Klauß, G. Korpala, R. Kawalla, W. Schillinger, and L. Schultz, Dynamic recrystallisation and precipitation behaviour of high strength and highly conducting Cu–Ag–Zr-alloys, Mater. Sci. Eng. A 597 (2014) 139-147.